ISSN: 0067-2904

New boroester compound derived from hydroxyaldehyde with some of its complexes and evaluation of biological and medical activities

Hawraa Abd Al- Jabbar K. and Asmaa Mohammed Noori Khaleel
Department of Chemistry, College of Science, University of Baghdad, Baghdad, Iraq

Received: 11/2/2024 Accepted: 7/10/2024 Published: 30/10/2025

Abstract

The ligand 4-formyl-2-methoxyphenyl dihydrogen borate (L) was synthesized through a 1:1 molar reaction between vanillin and boric acid. Additionally, the synthesis of metal complexes of L with Co(II), Ni(II), and Cu(II) was also described. All the synthesized compounds were described using spectroscopic methods like that FT-IR, ^{1}H NMR, UV-VIS. Also thermal analysis (TG),atomic absorption (AAS), elemental microanalysis (C.H.N), melting point (m.p.), magnetic susceptibility, molar conductivity and chloride measurements. The experiments determined that all the complexes were non-ionic compounds that did not dissociate into ions in solution. Additionally, the proposed molecular structures of these complexes were found to be octahedral in geometry. For C_1 (Co), C_2 (Ni), and C_3 (Cu), the complexes' magnetic moments were (3.54,2.73, and 2), indicating that each complex was paramagnetic. The synthesized compounds have good anti-microbial properties against *Escherichia coli (G-), Staphylococcus aureus (G+), and Candida albicans*. All synthesized compounds were evaluated as an anti-cancer agent against human thyroid cancer (FTCI33), the result showed that the copper complex was more effective compared to vanillin, ligand and its other complexes. The synthesized compounds were examined for anti-oxidant agents, the result showed that the ligand and nickel complex have more antioxidant activity than the other synthesized compounds.

Keywords: Vanillin, Boric acid, Antimicrobial, Anticancer, Antioxidant.

مركب بوروستر جديد مشتق من هيدروكسي ألدهيد مع بعض معقداته وتقييم الأنشطة البيولوجية والطبية

حوراء عبد الجبار خندان* ، أسماء محمد نوري خليل
قسم الكيمياء، كلية العلوم، جامعة بغداد، بغداد، العراق

الخلاصة

الليكاند 4-فورميل2-ميثوكسي فنيل ثنائي هيدروجين بورين(L) تم تحضيره بتفاعل الفانيلين مع حامض البوريك بالنسبة المولية (1:1)، بالإضافة الى المعقدات الفلزية مع Co(II) وNi(II) و Cu(II) تم وصفها ايضا, تم وصف جميع المركبات المحضرة باستخدام الطرق الطيفية مثل: ^{1}H NMR و FT-IR وUV-VIS . كذلك التحليل الحراري (TG) و الامتصاص الذري (AAS) والتحليل الدقيق للعناصر (C.H.N)وقياس درجة الانصهار (m.p.) والحساسية المغناطيسية والتوصيلية المولارية وقياس نسبة الكلورايد. حددت التجارب أن جميع المعقدات عبارة عن مركبات غير أيونية لا تتفكك إلى أيونات في المحلول. بالإضافة إلى ذلك، تم العثور على

*Email: omayveen@gmail.com

الهياكل الجزيئية المقترحة لهذه المعقدات لتكون ثماني السطوح في الهندسة. العزم المغناطيسي للمعقدات (3.54و2.73 و 2) لـ (C_1(Co)و (C_2(Ni و (C_3(Cu وهذا يدل على أن جميع المعقدات كانت بارامغناطيسية. تتمتع المركبات المحضرة بخصائص مضادة للميكروبات جيدة الإشريكية القولونية (G−)، المكورات العنقودية الذهبية (G+)، والمبيضات البيضاء. تم تقييم جميع المركبات المحضرة كعامل مضاد للسرطان ضد سرطان الغدة الدرقية لدى الإنسان (FTCI33) , اظهرت النتائج ان معقد النحاس كان اكثر فعالية مقارنة ب الفانيلين , الليكند وبقية المعقدات . بالإضافة إلى اختبار المركبات المحضرة كعوامل مضادة للأكسدة، أظهرت النتيجة أن الليكاند ومعقد النيكل لديهم نشاط مضاد للأكسدة أكثر من المركبات المحضرة الأخرى.

1. Introduction

Vanillin, a phenolic aldehyde with the chemical formula C8H8O3, is an organic compound (Figure 1). Its molecular structure features a combination of functional groups, including an ether group, a hydroxyl group, and an aldehyde group. As a flavoring for foods, drinks, and medications, synthetic vanillin is currently more commonly utilized than real vanilla extract. According to several studies, vanillin can affect the performance of antibiotics condition. Additionally, vanillin serves as a chemical intermediary in the production of pharmaceuticals, cosmetics, and other fine compounds. By 1970, over half of the global vanillin production was dedicated to the synthesis of other compounds. As of 2016, the uses of vanillin have spread to include flavoring and aromatic masking in medications, consumer and cleaning goods, livestock feed, and perfumes [1].

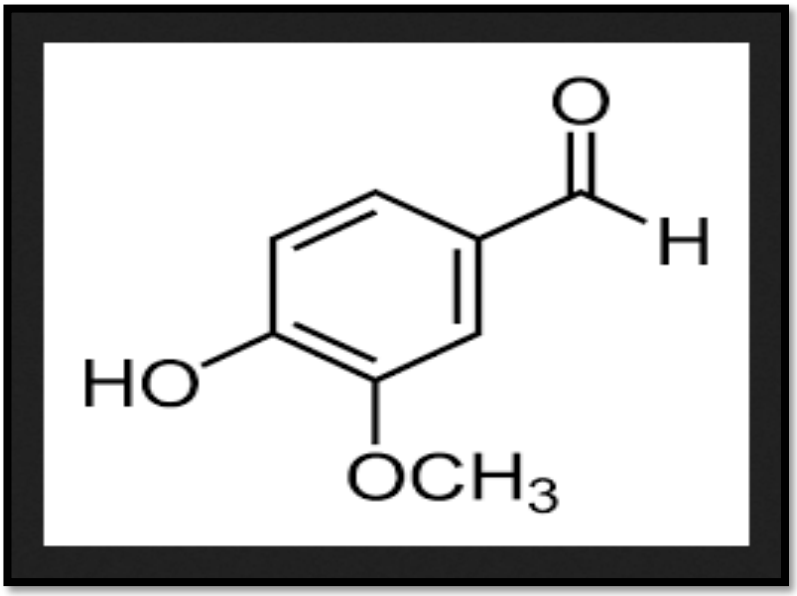

Figure 1: Structure of Vanillin

Both vanillin and ethyl vanillin are employed in the food industry. The key distinction between ethyl vanillin and vanillin is that ethyl vanillin contains an ethoxy group ($-O-CH_2CH_3$), while vanillin has a methoxy group ($-O-CH_3$). Vanillin is discovered as a natural product, glucovanillin, in vanilla beans. It can also be extracted from lignin in sulfite wastes treated with alkali, and from guaiacol, where its impurities are odourless [2].

4-hydroxy-3-methoxybenzaldehyde, commonly known as vanillin, is a small organic molecule which is safe to use and explored exponentially in many fields due to its exceptional properties [3]. From vanillin, several new transition metal complexes, including Schiff base ligand (HL) have been synthesized for Mn(II), Co(II),Cu(II), Ni(II), and Zn(II[4].

Boric acid, also known as boracic acid or orthoboric acid, is a very weak inorganic acid [5]. It is widely used in the pharmaceutical and chemical industries, serving as an antiseptic, as an eye wash solution, as a buffering agent and as an insecticide [6]. Additionally, boric acid finds extensive application in routine laboratory and research applications [7]. In pharmaceutical

formulations, boric acid has been used as an active component, a buffer, and an adjuvant or excipient. It additionally used in some foods, biocides, and cosmetics. Boric acid is frequently used in combination with glycerol, mannitol, or polyols, or other 1,2-diols [8].

The study aims to synthesise of borate ligand (4-formyl-2-methoxyphenyl dihydrogen borate) using the reaction of functional group (OH) of vanillin with boric acid in 1:1 mole ratio (Figure 2), also The metal complexes of the ligand with Co (II), Ni (II), and Cu (II) metal ions were synthesized by the reaction of the ligand with metal ions ($CoCl_2.6H_2O$, $NiCl_2.6H_2O$ and $CuCl_2.2H_2O$) in 2:1 mole ratio L:M. All the prepared compounds were characterized using physicochemical and spectral analyses. The antimicrobial against *Escherischia coli* (G-), *Staphylococcus aurus* (G+), and Candida albicans, antioxidant by using the DPPH Radical Scavenging Assay and anticancer against human thyroid cancer (FTCI33) activities were evaluated.

2. Experimental part

2.1. Materials

All chemicals used were supplied from (ReagentWorld.com, BDH (British Drug Houses), May and Baker (M&B), without additional purification.

Table 1: Inorganic , organic chemicals and solvents.

Compound	Formula	Purity	Supplier
Boric acid	$B(OH)_3$	99.9 %	BDH
Vanillin	$C_8H_8O_3$	99 %	ReagentWorld.com
Methanol	CH3OH	99.9%	Supelco
Acitic acid	CH_3COOH	99.8 %	BDH
Methylene chloride	CH_2Cl_2	99.5 %	BDH
Nickel(II)chloride Hexahydrate	$NiCl_2.6H_2O$	97%	M&B
Cobalt (II)chloride Hexahydrate	$CoCl_2.6H_2O$	97%	BDH
Copper(II)chloride Dehydrate	$CuCl_2.2H_2O$	98.5%	BDH

2.2. Methods

2.2.1. Synthesis of 4-formyl-2-methoxyphenyl dihydrogen borate (L)

The ligand (L) was synthesized by the reacting vanillin (1.23 g, 1.61734 m.mol) in 70ml of H2O with boric acid (0.5 g, 1.61734 m.mol) in (5ml) H2O (1:1 mole ratio). The mixture was refluxed for 20 hours, and the reaction was monitored using thin-layer chromatography (TLC) with an eluent [methylen chloride: acetic acid: methanol] [3.5:1.5:1ml] respectively. Part of the solvent (H2O) evaporated and the product was assembled by using both an icy bath and a crash, dried in an oven at 80 °C.

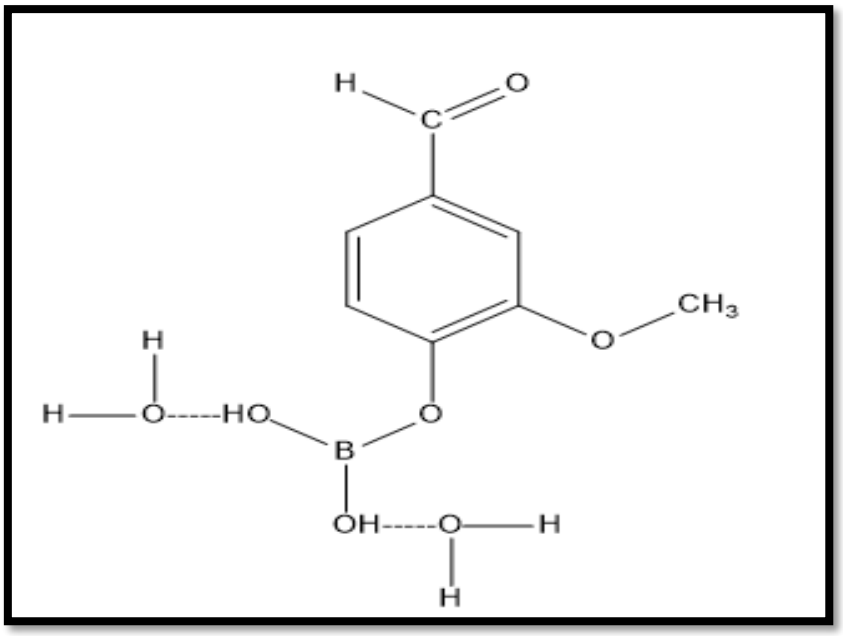

Figure 2: The structure of the ligand (L)

2.2.2. Synthesis of ligand complexes with Co (II), Ni (II) and Cu (II)) (C_1, C_2 and C_3)

A solution of $CoCl_2.6H_2O$ (0.2g, 0.8405mmole) in 2 mL distilled water was added to a solution of ligand (0.2859g, 1.2333mmole). The mixture was then heated to reflux for 5 hours. Part of the solvent was evaporated, and the product was collected using an ice bath and crashing, dried in an oven at 80 °C.

Using the same method as mentioned above, nickel and copper complexes were synthesized using (0.2g, 0.8414mmole) from $NiCl_2.6H_2O$ and (0.2g, 1.1727mmole) from $CuCl_2.2H_2O$ with (0.3295g, 1.4214mmole) and (0.4592g, 1.9809mmole) of ligand respectively as 2:1 mol ratio L: M.

2.2.3. The biological process

2.2.3.1. Antimicrobial activity

The antibacterial and antifungal properties of all synthesized compounds were evaluated using the well diffusion method using 10^{-3} M in aqueous water solutions against *Escherichia coli (G-), Staphylococcus aureus (G+), and Candida albicans*. The inhibition diameters were measured in order to assess antimicrobial activity.

2.2.4. Anticancer and antioxidant activity

To assess the cytotoxic effect, a 96 flat well micro-titer plate was used for the MTT cell viability assay. The cell-lines were seeded at a density of (1×10^4 – 1×10^6 cells / ml). Cells were treated with the studied compounds after 24 hours. The effectiveness of the anti-cancer for all synthesized compounds was studied depending on the literature [9], and absorbance at 575 nm was evaluated.

Antioxidant activity of synthesized compounds (Ligand, C_1, C_2 , and C_3) was assessed using of the DPPH Radical Scavenging Assay[10]. The DPPH radical was dissolved in a 1:9 (v/v) mixture of DMSO and methanol to provide a stock solution (0.1 mg/ml) of the DPPH radical.

3. Results and discussion

The physical and analytical data align with the proposed structures of all synthesized compounds (Table 1).

Table 2: Data of chemical and physical characteristics and formula of (L) and its metal complexes

Compound	Formula	Color	Yield (%)	Melting point (°C)	Molecular Wight (g/mol)	Calculated (Found)			Metal content (%)	Chloride content (%)
						C%	H%	N %		
Vanillin	$C_8H_8O_3$	White	-	81-83	152	63.15 (62.73)	5.26 (5.23)	-		
L	$C_8H_{13}O_7B$	White	86	152-156	231.81	41.41 (40.73)	5.60 (5.27)	-	-	-
C_1(Co)	$[C_{16}H_{18}O_{10}B_2CoCl_2]9H_2O$	Purple	85	126-130	683.533	28.08 (27.81)	5.26 (4.79)	-	7.38 (8.62)	9.65 (10.38)
C_2 (Ni)	$[C_{16}H_{18}O_{10}B_2NiCl_2]6H_2O$	Pale green	86	160 d	629.313	30.50 (30.84)	4.76 (4.97)	-	10.68 (9.32)	10.50 (11.28)
C_3 (Cu)	$[C_{16}H_{18}O_{10}B_2Cu_2Cl_4.2H_2O]\ 5H_2O$	Brown	64	200 d	786.692	24.40 (23.84)	4.60 (3.81)	-	15.74 (16.15)	17.31 (18.05)

d. decomposed

The chloride concentration of the complexes under investigation was ascertained using the Mohr method.

3.1. FT-IR spectroscopy of the ligand and its complexes

The FTIR analysis was conducted for the qualitative identification of synthesized compounds using KBr pellet for the ligands at the range [4000- 400 cm^{-1}] and CsI for complexes at the wave number range [4000-200 cm^{-1}]. [Table 3] and (Figures 3, 4, 5, 6, 7) present the data. The vanillin FT-IR spectral analysis(Figure 3) showed broad band of ν (OH) broad band appeared at (3178cm^{-1}) [11]. The stretching vibration of the carbonyl group showed up at (1666cm^{-1})[12]. The band that appeared at (1027cm^{-1}) was assigned to vibration stretching of the methoxy group [13, 14].

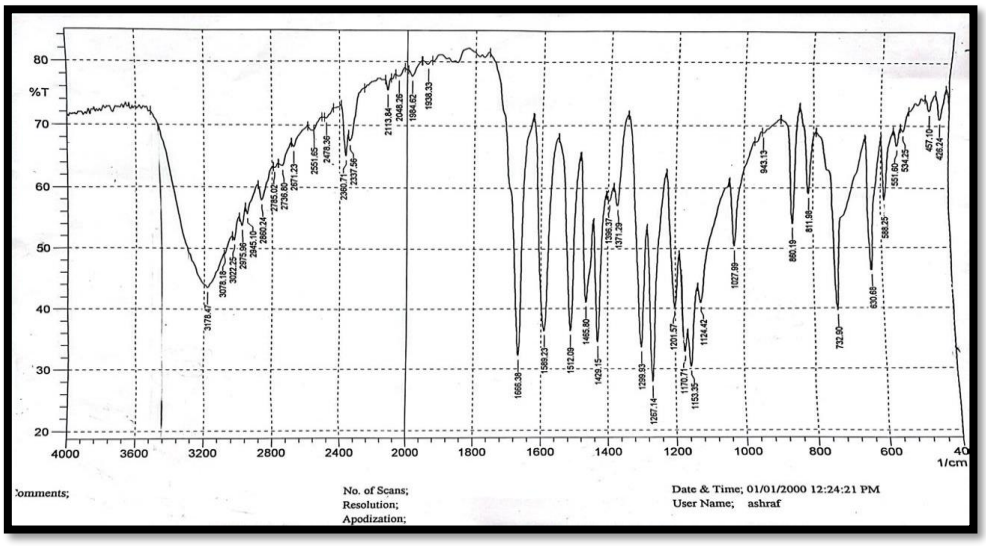

Figure 3: FT-IR spectrum of vanillin

The FTIR spectrum of L (Figure 4) displayed a shift in the stretching vibration of OH group, corresponding with the υ(OH) of vanillin, along with the emergence of new band appeared at (1454cm^{-1}), this band refer to υ B-O as a result of reaction with boric acid[15]. No change appeared in bands of υ C=O and stretching vibration of OCH_3 groups comparison with spectrum of vanillin [Table 3]. The hydrogen bond (between H_2O and B-OH) appeared at (3460cm^{-1}) [16].

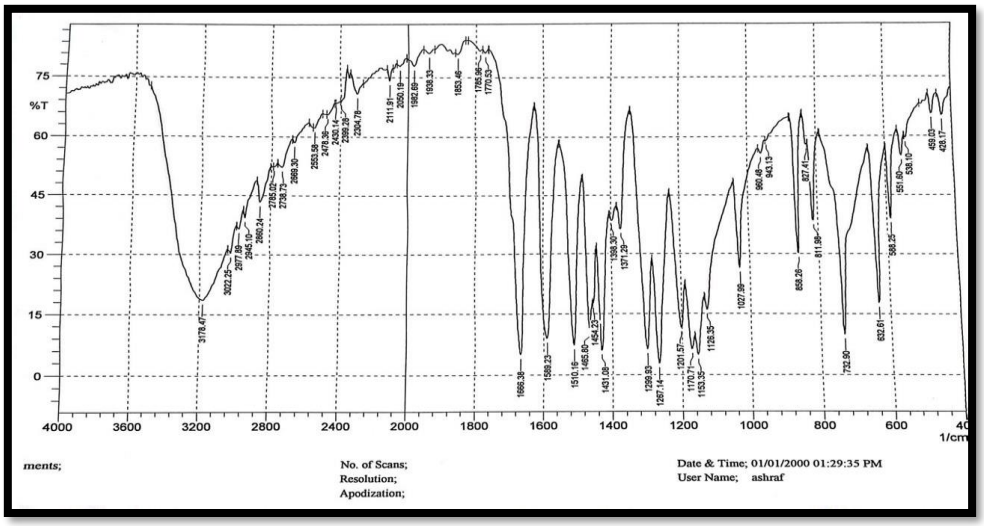

Figure 4: FT-IR spectrum of the ligand (L)

The spectra of the complexes exhibited bands in the range 3455-3474cm^{-1}, which are attributed to lattice H_2O [17]. In all complexes, the bands corresponding to υ OCH_3 change in frequency and appeared at (1049 – 1091cm^{-1}) (Table 3). This shift is related to the coordination of OCH_3 with metal ions via the oxygen atom. Another coordination with metal ions carried out through oxygen atom of B-O group, this coordination led to change in υ B-O (Table 3) as shown in Figure (5.a, and 7.a), Figure (5.b, 6 and 7.b). There was no change in stretching vibration of C=O groups for complexes this is because not coordination with metal ions. Low frequency bands appeared at range (491-503cm^{-1}) due to υ M-O (Table 3) [18, 19]. The spectra of complexes exhibited two types of υ M-Cl which have difference in frequency, one is bridge chloride in copper complex C_3, the second type is terminal chloride and this type existing in all complexes [20].

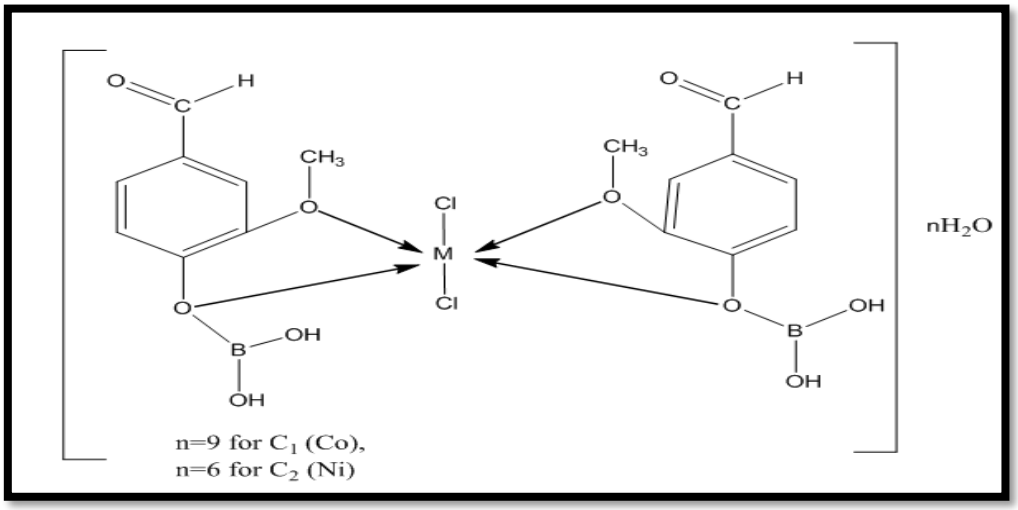

Figure 5:.a The suggested structure of cobalt (II) and nickel (II) complexes (C_1, C_2)

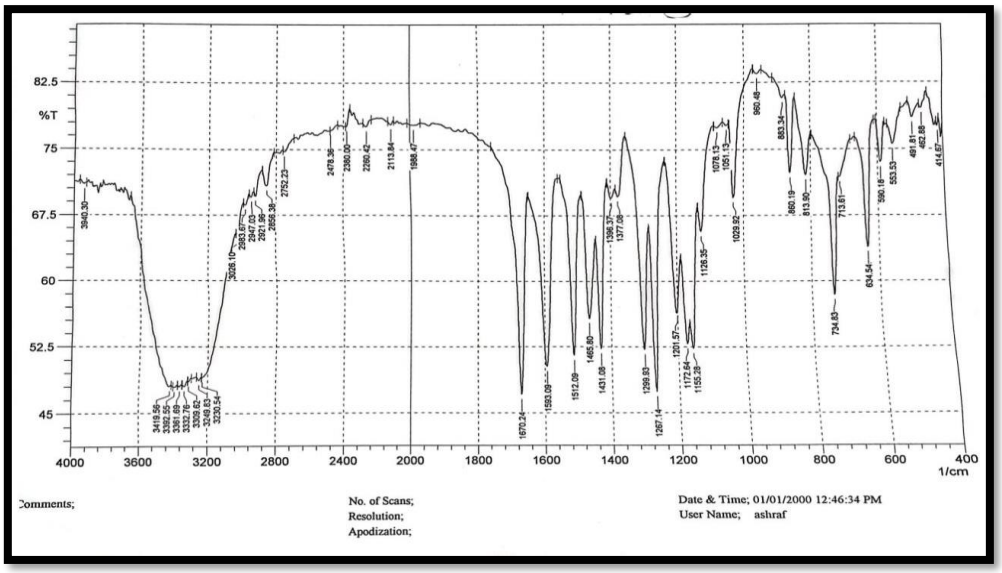

Figure- 5.b -FT-IR spectrum of the cobalt(II) complex C_1

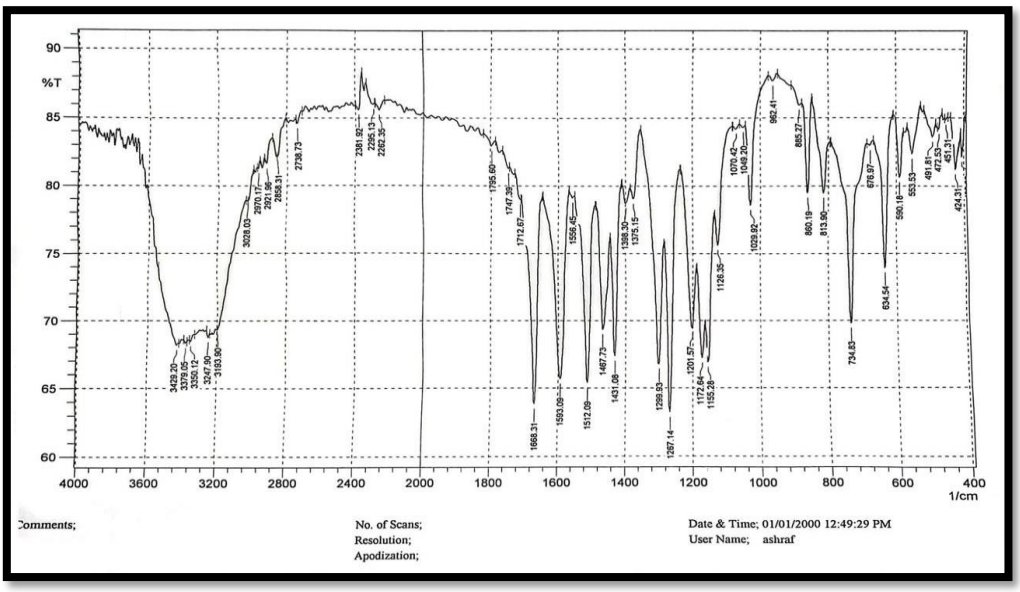

Figure 6: FT-IR spectrum of the Nnickel(II) complex C_2

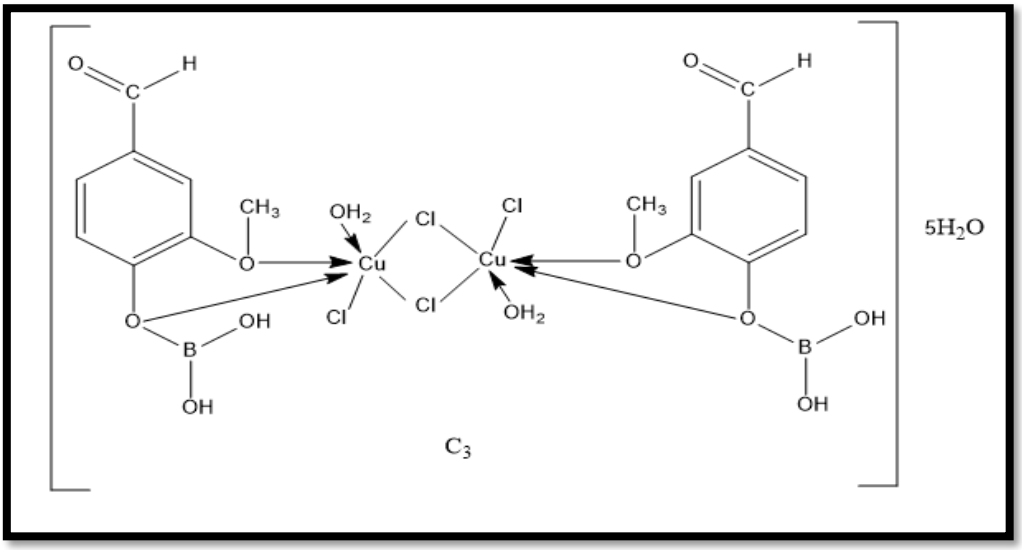

Figure 7: a The suggested structure of copper complex (C_3)

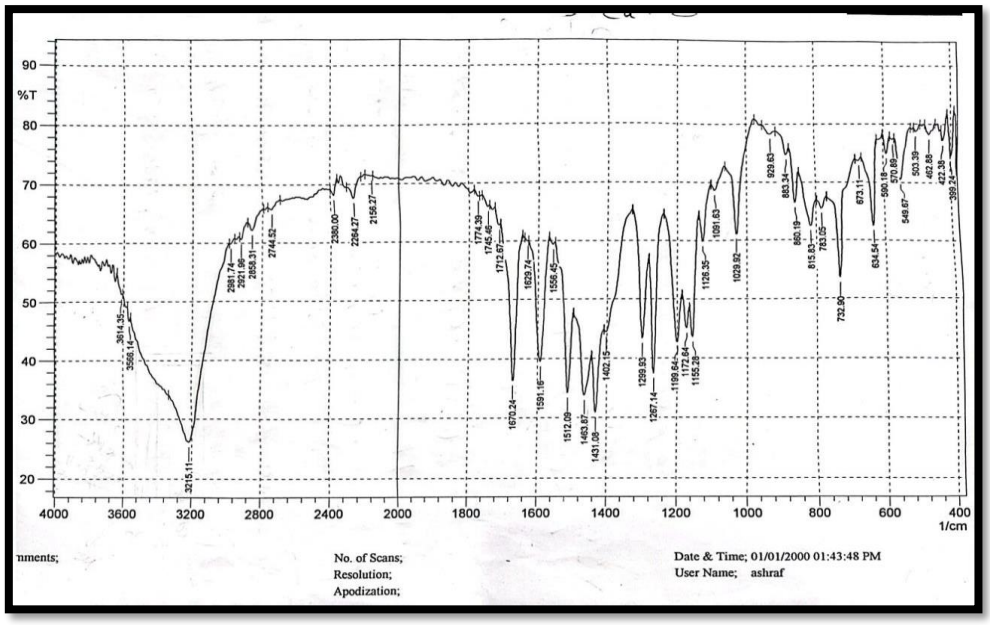

Figure 7: b FT-IR spectrum of the copper (II) complex C_3

Table 3: FT-IR spectral data of the ligand and it complexes

Symbol	ν OH cm^{-1}	νC=O cm^{-1}	ν B-O cm^{-1}	νOCH_3 cm^{-1}	H_2O Lattice (Coord.) Hydrogen bond cm^{-1}	νM-O cm^{-1}	νM-Cl cm^{-1}
Vanillin		1666	-	1027	-	-	-
L_1	3460	1666	1454	1027	3460	-	-
C_1(Co)	3419	1670	1465	1051	3455	491	302_a
C_2(Ni)	3429	1668	1467	1049	3470	491	316_a
C_3(Cu)	3415	1670	1463	1091	3474	503	335_a 268_b

a. Terminal
b. Bridging

3.2. ^{1}HNMR spectroscopy of ligand (L)

The 1HNMR spectrum of L displayed a signal at δ 2.5 ppm, corresponding to the chemical shift of the solvent d^6 -DMSO and the peak at (δ 3.42 ppm)4H,s attributed to H_2O protons as impurity [21, 22]. The positions of all the peaks' chemical shifts and their assignments are shown in (Table 4) depending on (Figures 8, and 9). The chemical shift for OCH3 is displayed at(δ 3.89 ppm)3H,m [23-25]. The proton of aromatic CH appeared at (δ 6.97-7.45 ppm) 3H, m [26-28]. The (L) spectrum showed a new peak at (δ10.27 ppm)2H, and this peak was attributed to the B-OH proton [29]. The peak appeared at (δ9.79 ppm)1H, referring to the aldehyde C-H proton [30, 31]. The results agree with the suggested structure of the ligand.

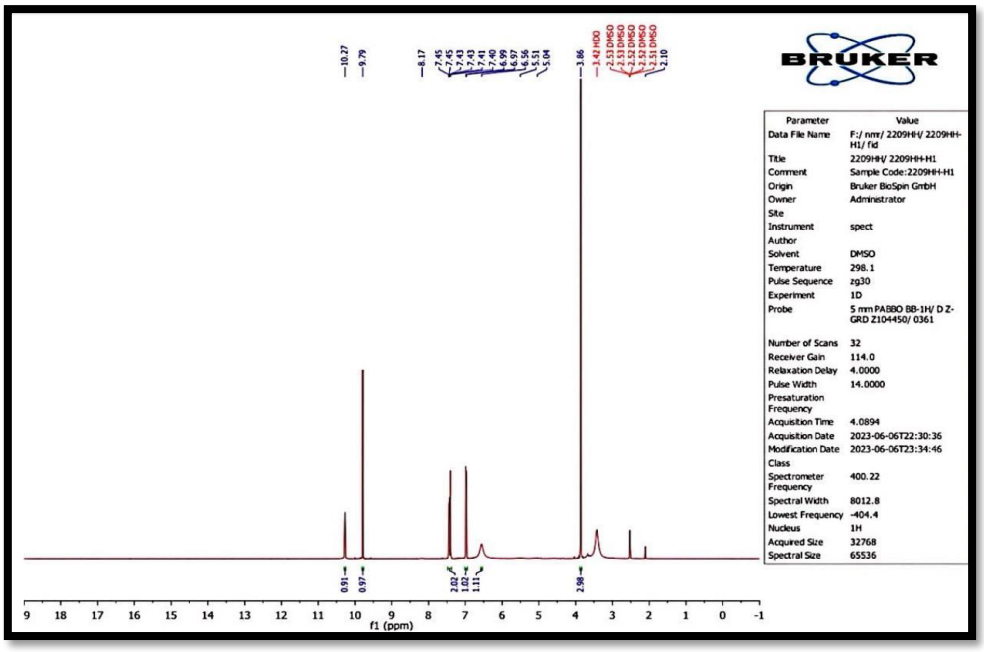

Figure 8: ^{1}H NMR spectrum of ligand

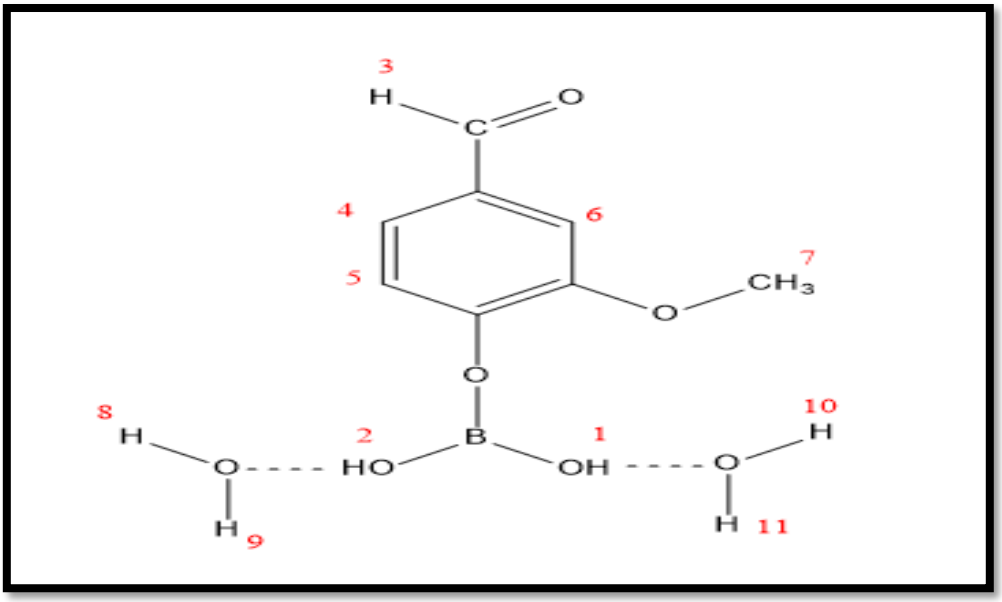

Figure 9: structure of the ligand (L)

3.3. Thermo gravimetric analysis (TGA)

Thermogravimetric (TG) analysis was performed under argon gas at a 10 C/min heating rate. And a 25–1200 oC temperature range. TG technique is used to prove the suggested structures as well as to study the thermal stabilities of the synthesized compounds.

The ligand was divided into three phases with percentages of 19.50, 43.01and 11.25%, which corresponds to the theoretical values of 20.11, 42.28and 10.82 for the partitioning. The curve also shows at what temperature the fracture occurred. Finally, the remaining part appeared without breakage (26.22%), and this residue indicates the stability of the studied compound. The thermogram of the ligand is presented in Figure 10.

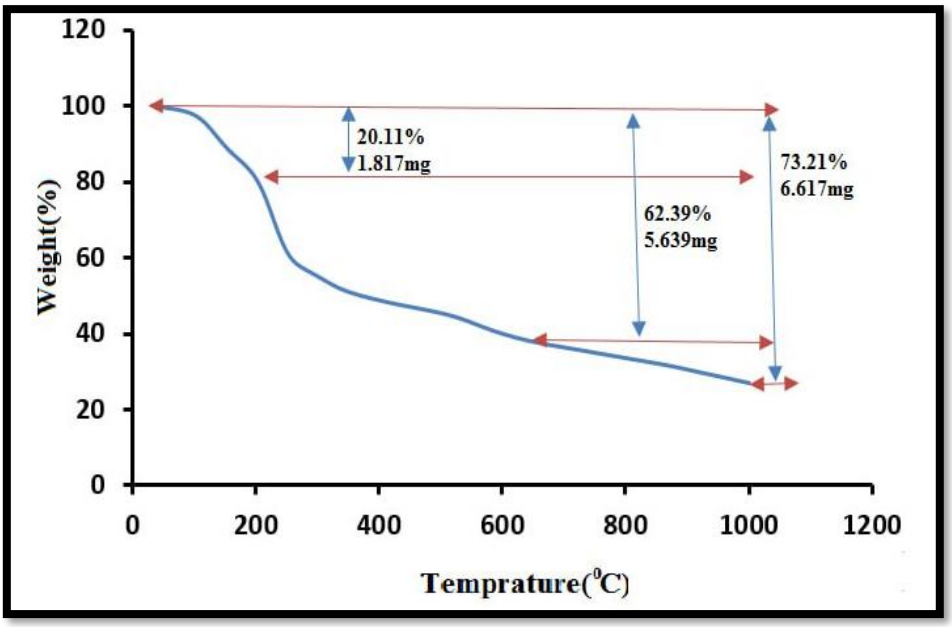

Figure 10: Thermogram of the Ligand (L)

The thermal decomposition of complexes (Figure 11, 12, 13) in three stages: (22.38, 44.59 and 19.86) % for C_1, (31.39, 52.31 and 6.92) for C_2 and (25.04, 43.80 and 21.89) for C_3 respectively. This division was carried out according to the temperatures listed in the [Table 5].

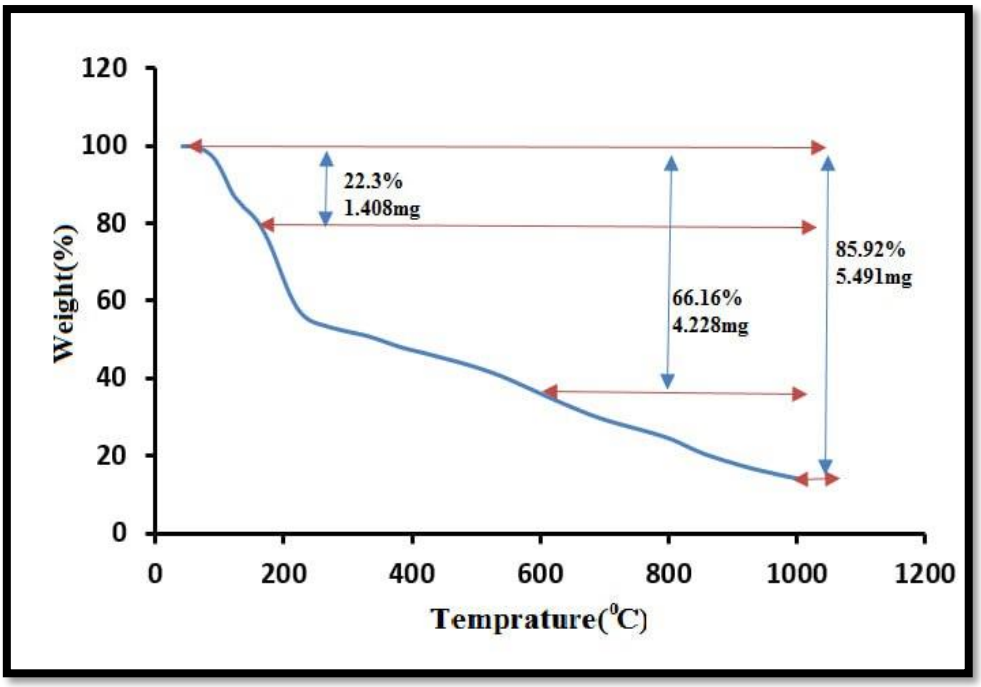

Figure 11: Thermogram of the cobalt complex (C_1)

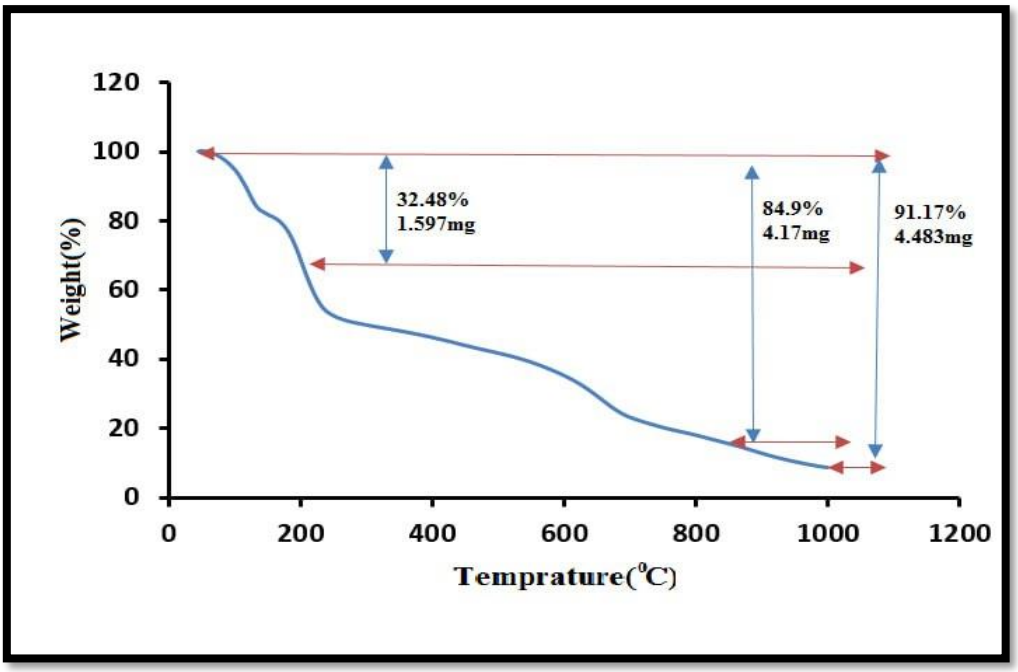

Figure 12: Thermogram of the nickel complex (C_2)

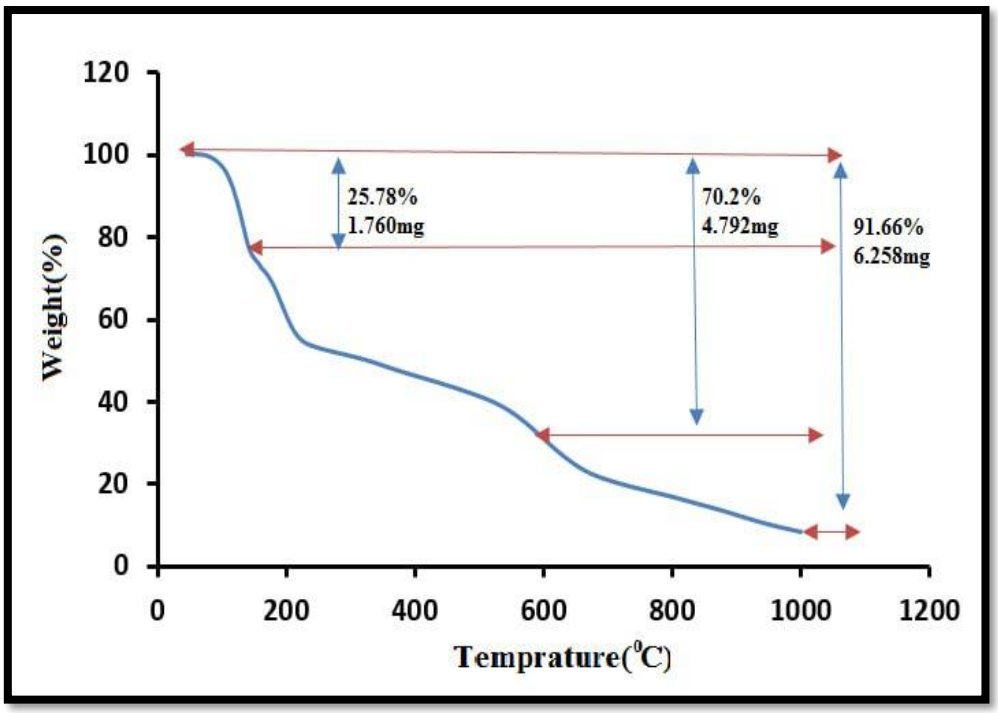

Figure 13: Thermogram of the copper complex (C_3)

The thermal stability of the ligand and its complexes was ranked as follows: ($L > C_1 > C_2 > C_3$). Thermal decomposition analysis was employed to confirm the structures where the information of degradation exhibits high agreed for found and calculated mass loss, which confirms the proposed structures of synthesized compounds.

Table 4: TGA data of the ligand and its complexes

Compounds	molecular weight or formula g/mole	Step	Temperature rang of the decomposition (°C)	Suggested loss formula	Mass loss (%) Calculated	Found
L_1	$C_8H_{13}O_7B$ 231.81	1	25-350	$2H_2O+0.3OCH_3$	19.50	20.11
		2	350-820	$0.7OCH_3+0.75C_6H_3CHO$	43.01	42.28
		3	820-1050	$0.25\ C_6H_3CHO$	11.25	10.82
		Residue	1050	H_2BO_3	26.22	26.79
C_1	$[C_{16}H_{18}O_{10}B_2CoCl_2]9H_2O$ 683.533	1	25-250	$8.5H_2O$	22.38	22.3
		2	250-800	$0.5H_2O+Cl_2+C_6H_3+2CHO+OCH_3+H_2BO_3$	44.59	43.86
		3	800-1040	$C_6H_3+ H_2BO_3$	19.86	19.79
		Residue	1040	$Co+ OCH_3$	13.15	14.08
C_2	$[C_{16}H_{18}O_{10}B_2NiCl_2]6H_2O$ 629.313	1	25-310	$6H_2O+Cl_2+0.6\ OCH_3$	31.39	32.48
		2	310-890	$0.4\ OCH_3+2C_6H_3+2CHO+ OCH_3+H_2BO_3+OH$	52.31	52.42
		3	890-1060	HBO_2	6.92	6.27
		Residue	1060	Ni	9.32	8.83
C_3	$[C_{16}H_{18}O_{10}B_2Cu_2Cl_4.2H_2O]\ 5H_2O$ 786.692	1	25-290	$7H_2O+Cl_2$	25.04	25.78
		2	290-840	$2C_6H_3+2CHO+ OCH_3+H_2BO_3+ H_2BO_2$	43.80	44.42
		3	840-1070	$0.7OCH_3+CuO+ Cl_2$	21.89	21.46
		Residue	1070	$0.3OCH_3+Cu$	9.25	8.34

3.4. UV-Vis spectroscopic studies

The electronic spectra of synthesized compounds were recorded at room temperature in distilled water at a concentration of 10^{-3}M. All the details of the spectra are listed in [Table 6]. The spectrum of L (Figure 14.a) exhibited high-intensity bands in the region of 277 nm (36101 cm^{-1}) and 308 nm (32467 cm^{-1}), which were assigned to the π -π* transition [32, 33]. The spectrum of the ligand did not exhibit a band of n -π* because this band is forbidden[34].

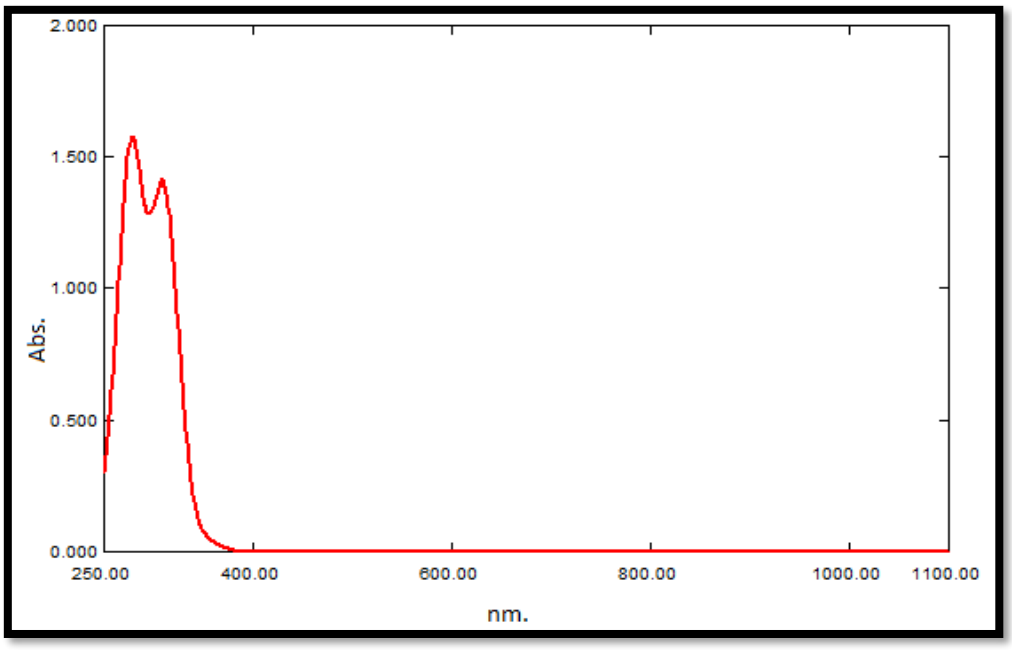

Figure 14: a UV-Vis spectrum of Ligand

Due to coordination with the metal ion, the position of the π -π* transition (intra ligand) shifted in the spectrum of Co (II) complex (Figure 14.b). Two bands were appeared at 483nm (20744cm^{-1}), 903nm (11013 cm^{-1}), which refer to $^4T1g \rightarrow {}^4T1g(p)$ (υ3) and $^4T1g — {}^4A2g(\upsilon_2)$ transitions, respectively [35]. The magnetic moment of the cobalt complex (C_1) was 3.54 BM, and this value of Meff agreed with octahedral geometry [36].

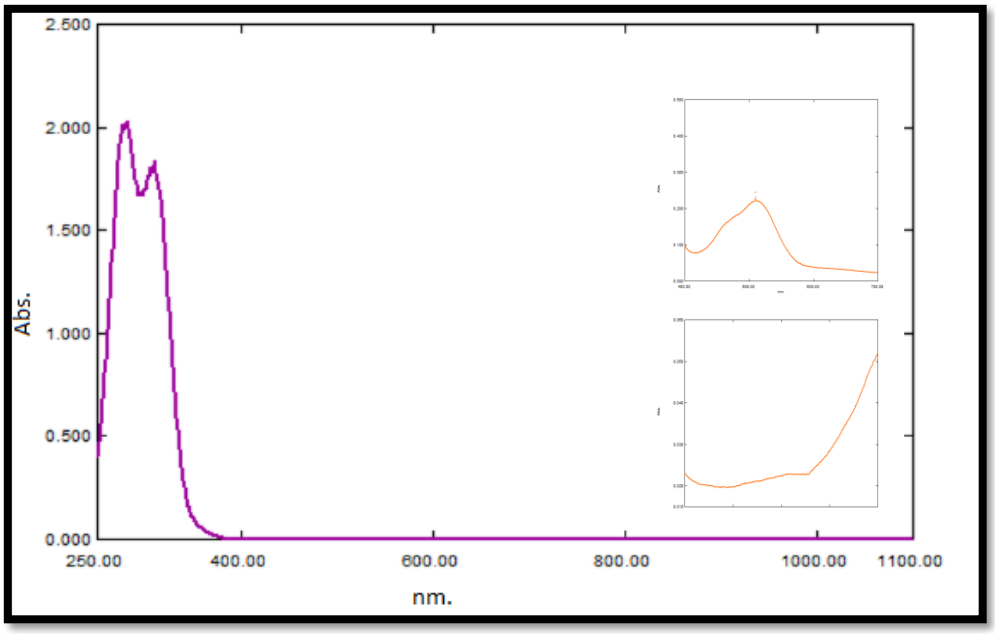

Figure 14: b UV-Vis spectrum of Cobalt complex (C_1)

The nickel Complex Spectral Analysis (Figure 14.c) exhibited a shift in the location of the π -π* transition(intra ligand). The band of C_2 at 689 nm (14535) cm^{-1} refer to $^3A_1g \rightarrow {}^3T_1g(\upsilon_2)$ transition [37]. The nickel complex (C_2) had a magnetic moment of 2.73 BM, and the value of M_{eff} demonstrated octahedral geometry[38].

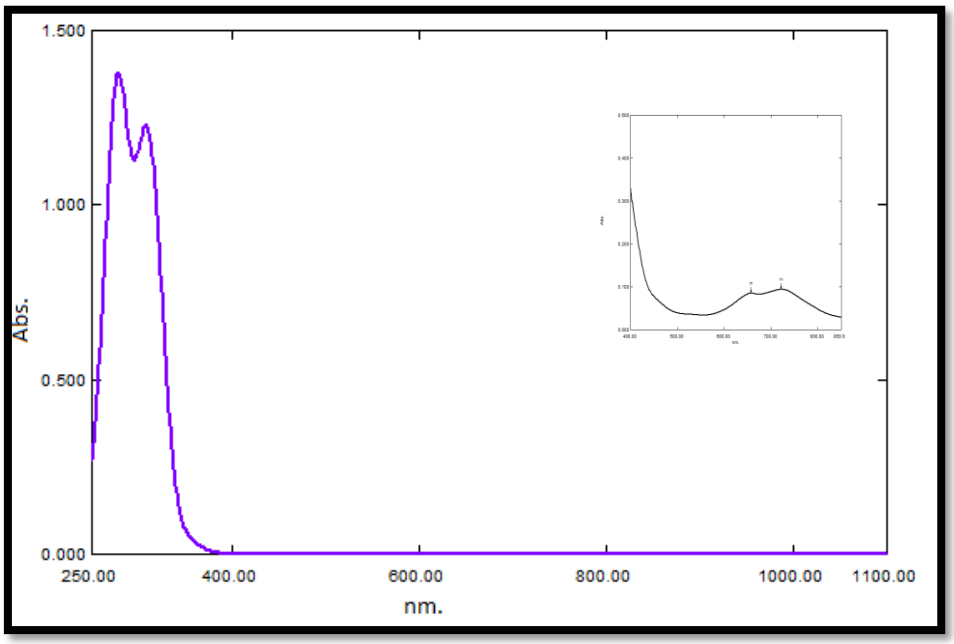

Figure 14: c UV-Vis spectrum of Nickel complex (C_2)

The spectrum of Cu (II) complex is presented in (Figure 14.d), displayed a shift in the π - π* transition. The electronic spectrum of C_3 showed a band at 804nm (12437cm^{-1}) that also due to the $^2B_1g \rightarrow {}^2A_1g(H)$ (υ_1) transition [26]. The magnetic moment of the copper complex (C_3) was 2 BM, and the value of M_{eff} demonstrated octahedral geometry[39]. The molar conductivity measurements of C_1, C_2, and C_3 complexes in distilled water showed that all complexes were non-electrolyte [40].

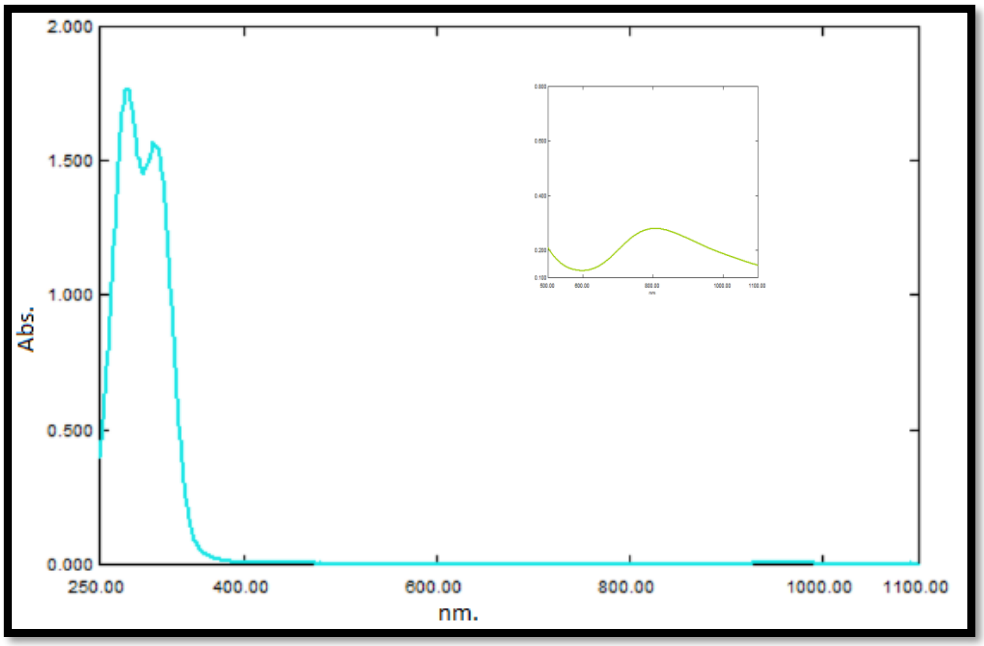

Figure 14: d UV-Vis spectrum of Copper complex (C_3)

The magnetic properties of all complexes are paramagnetic. Cobalt and nickel complexes did not show an orbital coupling. The M_{eff} experimental value of the copper complex was greater than the theoretical one and this indicate existence orbital coupling.

Table 5: Electronic transitions of the ligand and its complexes, proposed geometry, molar conductivity, and magnetic susceptibility

Comp.	Band locations nm(cm-1)	The Assignment	Molar conductivity ($S.cm^2.mol^{-1}$) in H_2O	Experimental(B.M.)	Theortical (B.M.)	Suggested geometry
L1	277(36101) 308(32467)	(π -π*) (π -π*)	-	-	-	-
C_1 (Co)	282(35460) 310(32258) 483(20744) 908(11013)	Intra ligand Intra ligand $^4T_1g \rightarrow {}^4T_1g(P)$ (υ_3) $^4T_1g \rightarrow {}^4A_2g$ (υ_2)	9.02	3.54	3.8	Octahedral
C_2 (Ni)	309(32362) 279(35842) 689(14535)	Intra ligand Intra ligand $^3A_1g \rightarrow {}^3T_1g(\upsilon_2)$	7.27	2.73	2.8	Octahedral
C_3 (Cu)	306(32679) 281(35587) 804(12437)	Intra ligand Intra ligand $^2B_1g \rightarrow {}^2A_1g(H)$ (υ_1)	3.53	2	1.7	Octahedral

3.5. Anti-cancer activity

The cytotoxic effects of vanillin, the ligand, and the complexes on thyroid cancer cells (FTCI33) were evaluated using the 3-(4, 5-dimethylthiazol-2-yl)-2, 5-diphenyltetrazolium bromide (MTT). With an IC_{50} of 119µg/ml, the percentage of cancer cells killed by vanillin was (100-55.208=44.792) at 400 µg/ml and (100- 94.675=5.325) at 25 µg/ml. The percentage of viable cancer cells was (55.208-94.675%) (Figure 15). Vanillin possesses less effect on killing normal cells than cancer cells (FTCI33). For (400–25) g/ml, the percentage of viable cells was (74.884–94.637) %, with an IC_{50} of 123.9µg/mL and a p-value < 0.0001 [Table 7].

Table 6 : Cytotoxicity effects of vanillin on FTCI33 and Hdfn cells after 24 hours of incubation at 37 °C

Cell line	Concentration (µg/ml)					IC_{50} (µg/ml)	P value
	400.00	200.00	100.00	50.00	25.00		
FTCI33	55.208± 1.862	63.117± 2.552	77.623± 2.411	86.561± 2.084	94.675± 0.601	119.0	<0.0001
Hdfn	74.884± 5.007	86.072± 3.076	90.084± 1.049	93.865± 1.104	94.637± 0.481	123.9	

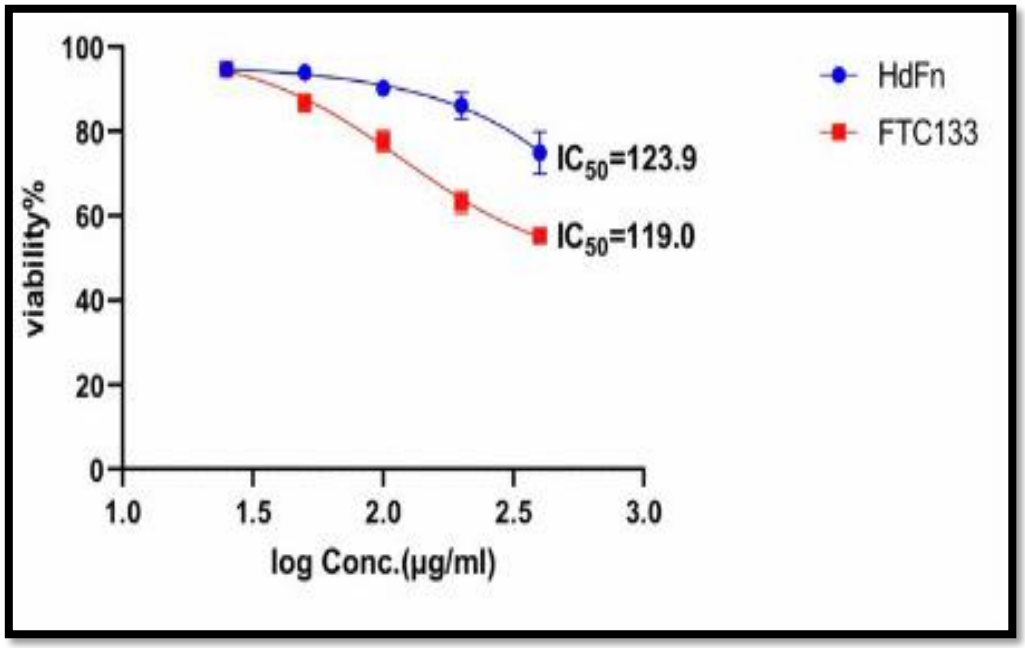

Figure 15: The cytotoxicity of vanillin on FTCI33cells (Log for the original concentration), after 24 hours of incubation at 37 °C.

For the ligand, the percentage of viable cancer cells was (39.390-82.484) µg/ml. This means that the percentage of killing for cancer cells was (100-39.390=60.61) at 400 µg/ml and (100-82.484=17.516) at 25µg/ml and the IC_{50} =84.01 µg/ml (Figure 16). While the effect of ligands on normal cells (Hdfn) was lower killing effect compared with cancer cells in which the percentage of the viable cells ranging from 70.794 to 94.328). This was accompanied by a p-value < 0.0001 and an IC_{50} of 105.2 µg/ml [Table 8].

Table 7 : Cytotoxicity effects of ligand on FTCI33and Hdfn cells after 24 hours incubation at 37 °C

Cell line	Concentration (µg/ml)					IC_{50} µg/ml	P value
	400.00	200.00	100.00	50.00	25.00		
FTCI33	39.390± 2.955	47.569± 5.303	58.564± 2.559	73.148± 1.445	82.484± 4.545	84.01	<0.0001
Hdfn	70.794± 6.102	82.870± 1.632	86.921± 1.819	93.094± 2.383	94.328± 1.408	105.2	

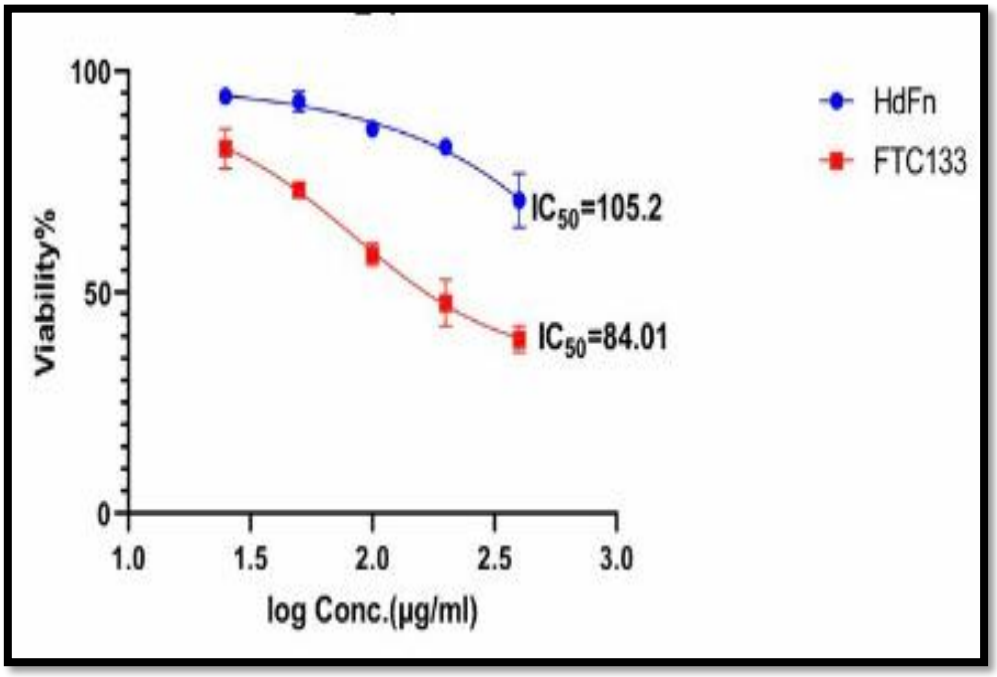

Figure 16: the cytotoxicity of ligands on FTCI33cells (Log for the original concentration), after 24 hours of incubation at 37 °C.

For the complexes, the results of the C_1, C_2 and C_3 indicated that the percentage of viable cancer cells was (51.427-94.560), (35.648-76.118) and (26.195-68.364) % respectively at (400-25) µg/ml. This means that the percentage of killing for cancer cells was (100-51.427=48.573) at 400 µg/ml and (100-94.560=5.44) at 25µg/ml and the IC_{50} =134.9 µg/ml (Figure 17) for cobalt complex (C_1). The percentage of nickel complex (C_2) was (100-35.648=64.352) at 400 µg/ml and (100-76.118=23.882) at 25 µg/ml, and the IC_{50} = 121.7µg/ml (Figure 18). The percentage of copper complex (C_3) was (100-26.195=73.805) at 400 µg/ml and (100-68.364=31.636) at 25 µg/ml, and the IC_{50} = 32.5 µg/ml (Figure 19). While the effect of complexes on normal cells (Hdfn) was a lower killing effect compared with cancer cells in which the percentage of the viable cells were (68.943- 94.270), (68.480- 94.135) and (51.427- 88.233) % at (400 - 25) µg /ml for C_1 and C_2 and C_3 respectively, with p-value < 0.0001 and IC_{50} for the complexes were (153.5, 155.2 and 97.3) µg/ml respectively (Table 9, 10 and 11).

Table 8 : Cytotoxicity effects of Co complex (C_1) on FTCI33and Hdfn cells after 24 hours incubation at 37 °C

Cell line	**Concentration (µg/ml)**					**IC_{50} µg/ml**	**P value**
	400.00	**200.00**	**100.00**	**50.00**	**25.00**		
FTCI33	51.427± 3.588	64.043± 7.351	82.446± 3.653	93.171± 1.116	94.560± 0.578	134.9	<0.0001
Hdfn	68.943± 1.686	76.273± 1.894	84.529± 4.155	94.444± 1.288	94.270± 0.852	153.5	

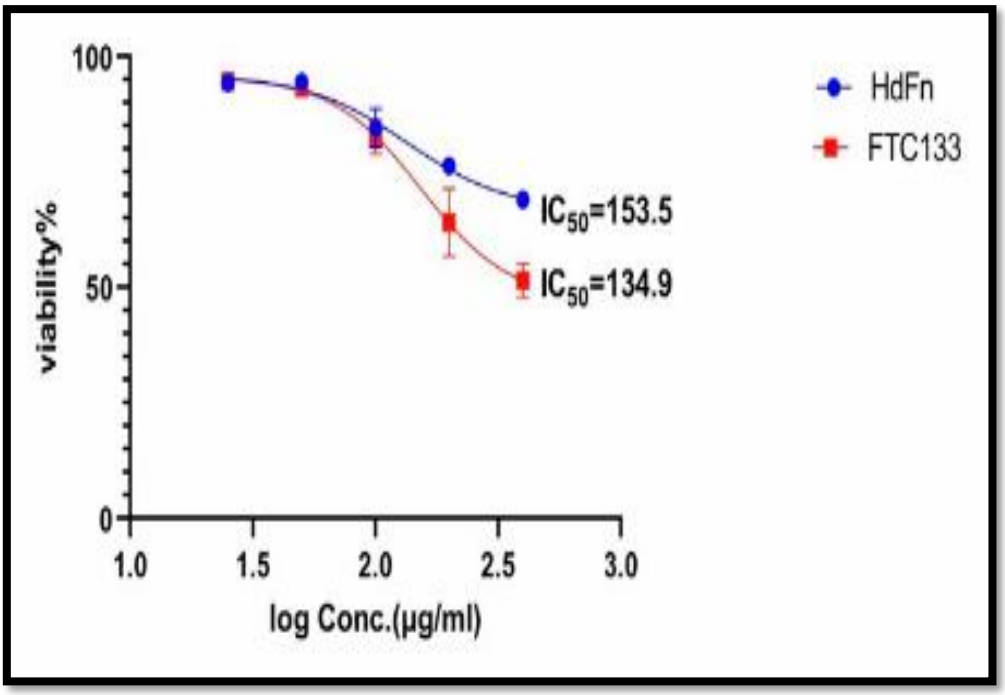

Figure 17: The cytotoxicity of Co complex (C_1) on FTCI33cells (Log for the original concentration), after 24 hours of incubation at 37 °C.

Table 9 : Cytotoxicity effects of Ni complex (C_2) on FTCI33and Hdfn cells after 24 hours incubation at 37 °C

Cell line	Concentration (µg/ml)					IC_{50} µg/ml	P value
	400.00	200.00	100.00	50.00	25.00		
FTCI33	35.648± 3.708	48.187± 1.011	57.060± 3.348	68.711± 2.239	76.118± 1.562	121.7	<0.0001
Hdfn	68.480± 2.257	74.460± 4.078	83.063± 1.718	87.924± 2.960	94.135± 1.447	155.2	

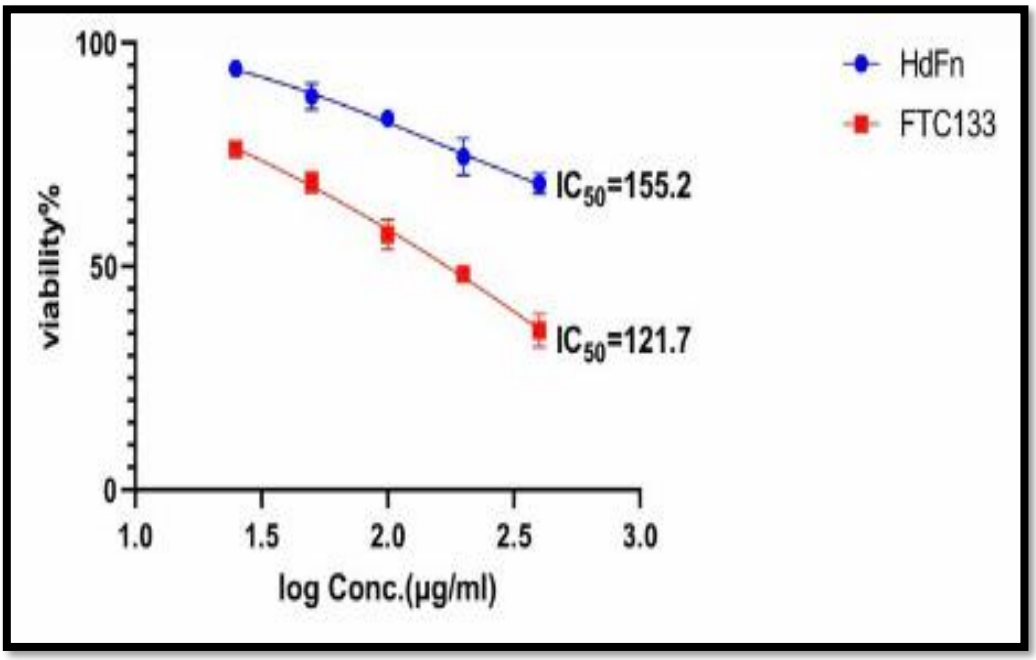

Figure 18: the cytotoxicity of Ni complex (C_2) on FTCI33cells (Log for the original concentration), after 24 hours of incubation at 37 °C.

Table 10 : Cytotoxicity effects of Cu complex(C_3) on FTCI33and Hdfn cells after 24 hours incubation at 37 °C

Cell line	Concentration (µg/ml)					IC_{50} µg/ml	P value
	400.00	200.00	100.00	50.00	25.00		
FTCI33	26.195± 1.958	36.034± 2.905	44.560± 1.273	53.279± 1.951	68.364± 4.637	32.5	<0.0001
Hdfn	51.427± 4.193	62.538± 1.686	67.631± 1.226	76.929± 1.717	88.233± 2.604	97.3	

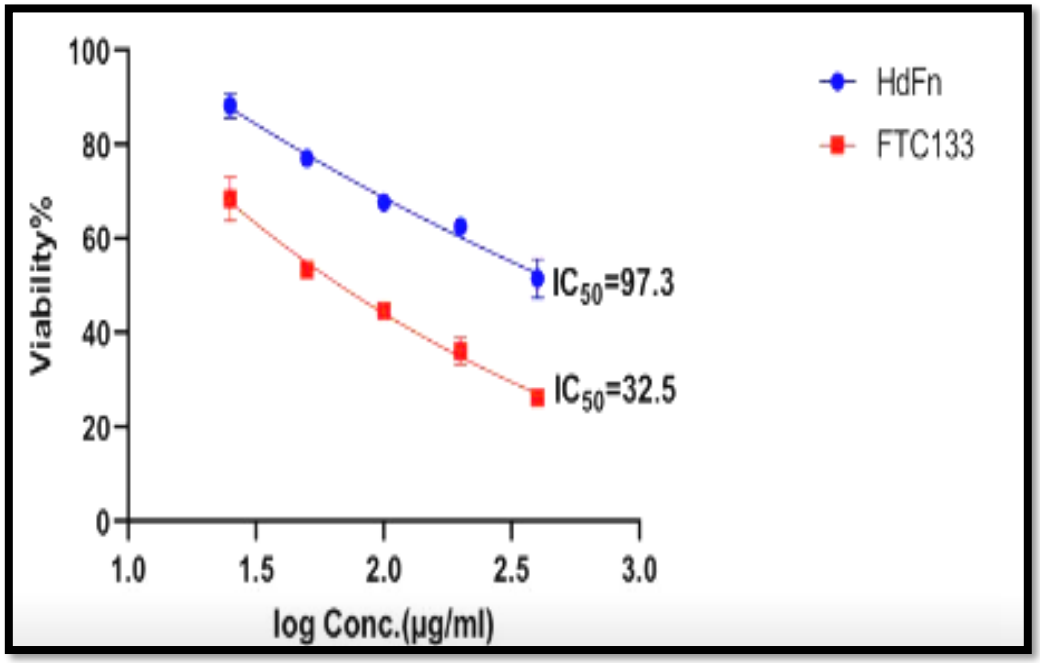

Figure 19: the cytotoxicity of Cu complex (C_3) on FTCI33cells (Log for the original concentration), after 24 hours of incubation at 37 °C.

Through the IC_{50}, The anticancer abilities of both the ligand and its complexes were more than the essential material (vanillin) and the order of activity was C_3>C_2>L>C_1>Vanillin, these results also showed that the synthesized compounds have less effect on healthy cells (Hdfn) and strong effect on FTCI33 cells.

3.6. Anti-oxidant activity

The antioxidant scavenging activity of certain synthesized compounds is presented in Table

Table 11: scavenging activity of some of the synthesized compounds (L, C_1, C_2, and C_3)

Comp.	Scavenging %				
	Conc. (12.5 µg/ml)	Conc. (25 µg/ml)	Conc. (50 µg/ml)	Conc. (100 µg/ml)	Conc. (200 µg/ml)
L	24.46	40.54	52.19	63.85	77.93
C_1 (Co)	15.77	24.61	25.42	42.66	56.48
C_2 (Ni)	28.97	40.81	54.47	65.74	79.05
C_3 (Cu)	17.63	30.55	44.09	52.43	65.20

The scavenging activity of L and C_2 in concentrations of 25, 50 and 100 µg/ml was less than that of ascorbic acid due to their statistically significant differences from ascorbic acid. However, at a concentration 200 there was no significance difference between (L,C_2) and ascorbic acid, suggesting that ligand and nickel complex (C_2) exhibit greater active than

ascorbic acid in this concentration. This may indicate that as the concentration of a component increases, its scavenging activity or antioxidant capacity. The other complexes C_1 and C_3 have significance difference in all concentrations comparison with ascorbic acid, (Figure 20).

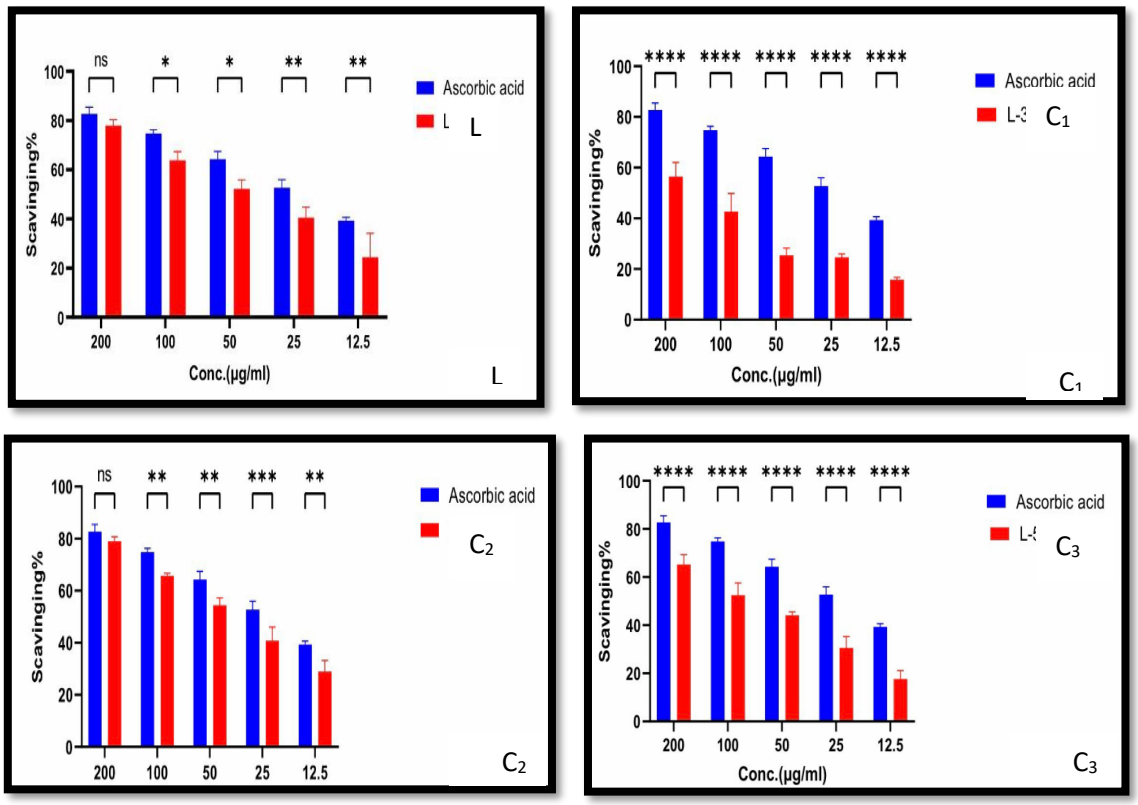

Figure 20: scavenging activity assay by DPPH of (L,C_1,C_2, and C_3)

3.7. Biological Activity (Antimicrobial Activity)

The antimicrobial activity was investigated for the ligand and its complexes using the 10^{-3} M by diffusion method along with water as a solvent. The antibacterial and antifungal activity of the synthesized compounds was examined against *Staphylococcus aureus (G+), E. coli (G-), and candida albicans*. From the results, the ligand was less active than its complexes (Table 12) and this is because of metal ions effect on microorganisms membrane. The order of activity was C_1> C_3> C_2>L on *Staphylococcus aureus* at inhibition zone (23 > 12 > 11 >10) mm, C_3> C_1> C_2>L on *E. coli* depending on inhibition zone (31 > 20 > 18 >9) mm, *and* C_3> C_1> C_2>L on *candida albicans* at inhibition zone (32 > 29 > 17 >14) mm respectively. Figures 21 and 22 show the inhibition zone for tested compounds.

Table 12: The investigated chemicals' biological activities in (10^{-3} M)

Comp.	Staphylococcus aureus (G+) (mm)	E. coli (G-) (mm)	candida albicans
L	10	9	14
C_1(Co)	23	20	29
C_2(Ni)	11	18	17
C_3(Cu)	12	31	32

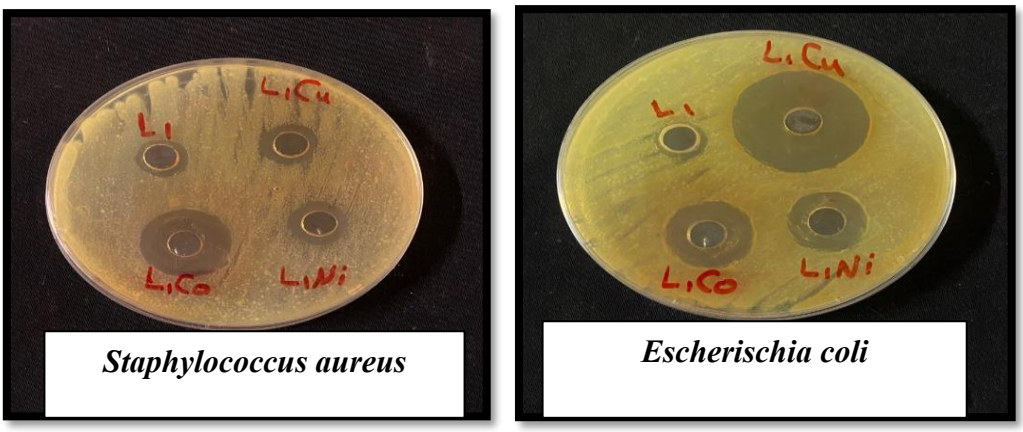

Figure 21: The inhibition zone for the ligand and its complexes against Staphylococcus aurus (G+)and E.coli (G-)

Figure 22: The inhibition zone for the ligand and its complexes against Candida albicans

Conclusion

A new ligand was synthesized through the reaction of vanillin with boric acid, and its metal complexes with Co(II), Ni(II), and Cu (II), were also synthesized in a 2:1 mole ratio (L: M). Every compound that was created was described, additionally, the proposed structure makes use of spectral and physicochemical methods like FT-IR, 1H NMR, and UV-VIS. Also thermal analysis (TG), atomic absorption (AAS), elemental microanalysis (C.H.N), melting point (m.p.), magnetic susceptibility, molar conductivity and chloride measurements. The results indicated that all complexes exhibited non-electrolyte behavior and octahedral geometry. Furthermore, all of the produced compounds exhibited high antimicrobial activity against Escherichia coli (G-), Staphylococcus aureus (G+), and Candida albicans, as demonstrated by the biological results. The synthesized compounds were tested as anticancer in vitro, the copper complex has the strongest activity against human thyroid cancer (FTCI33) cells than vanillin, ligand,and other complexes. Also, the results showed that the ligand and nickel complex have more antioxidant activity than the other synthesized compounds.

References

[1] I. S. Pratt, "Global harmonisation of classification and labelling of hazardous chemicals," *Toxicology letters,* vol. 128, no. 1-3, pp. 5-15, 2002.

[2] B. R. Chavda , "Coordination behavior of dinuclear silver complex of sulfamethoxazole with solvent molecule having static rotational disorder: Spectroscopic characterization, crystal

structure, Hirshfeld surface and antimicrobial activity," *Journal of Molecular Structure,* vol. 1228, p. 129777, 2021.

[3] V. Sharma and S. W. Ali, "Nanoarchitectonics of vanillin-metal complexes as eco-friendly multifunctional agents on cellulosic fabric," *Journal of Inorganic and Organometallic Polymers and Materials,* vol. 33, no. 7, pp. 1932-1945, 2023.

[4] G. I. Saleh, H. Mohammed, and Z. M. Mustafea, "Synthesis, characterization, anti-bacterial activity study of vanillin schiff base complexes," *Kirkuk Journal of Science,* vol. 16, no. 4, pp. 13-20, 2021.

[5] R. Pal, "Boric acid in organic synthesis: scope and recent developments," *ARKIVOC: Online Journal of Organic Chemistry,* vol. 2018, 2018.

[6] C. P. Cooper, L. Polonec, and C. A. Gelb, "Women's knowledge and awareness of gynecologic cancer: a multisite qualitative study in the United States," *Journal of Women's Health,* vol. 20, no. 4, pp. 517-524, 2011.

[7] S. S. Gujral, "UV-Visible spectral analysis of boric acid in different solvents: a case study," *International Journal of Pharmaceutical Sciences and Research,* vol. 6, no. 2, p. 830, 2015.

[8] A. Lopalco, A. A. Lopedota, V. Laquintana, N. Denora, and V. J. Stella, "Boric acid, a Lewis acid with unique and unusual properties: formulation implications," *Journal of Pharmaceutical Sciences,* vol. 109, no. 8, pp. 2375-2386, 2020.

[9] A. A. HUSSEIN, S. I. ALBARAZANCHI, and A. F. AL-SHANON, "Evaluation of anticancer potential for L-glutaminase purified from Bacillus subtilis," *International Journal of Pharmaceutical Research (09752366),* vol. 12, no. 1, 2020.

[10] M. Patel Rajesh and J. Patel Natvar, "In vitro antioxidant activity of coumarin compounds by DPPH, Super oxide and nitric oxide free radical scavenging methods," *Journal of advanced pharmacy education & research,* vol. 1, no. 1, pp. 52-68, 2011.

[11] A. Fatoni, P. L. Hariani, H. Hermansyah, and A. Lesbani, "Synthesis and characterization of chitosan linked by methylene bridge and schiff base of 4, 4-diaminodiphenyl ether-vanillin," *Indonesian Journal of Chemistry,* vol. 18, no. 1, pp. 92-101, 2018.

[12] H. Reyes, M. C. García, B. M. Flores, H. López-Rebolledo, R. Santillán, and N. Farfán, "Synthesis, NMR and X-ray diffraction analysis of boron complexes derived from hydroxychalcones," *Journal of the Mexican Chemical Society,* vol. 50, no. 3, pp. 106-113, 2006.

[13] K. S. Kuamr, C. P. Varma, V. Reena, and K. Aravindakshan, "Synthesis, characterization, cytotoxic, anticancer and antimicrobial studies of novel Schiff base ligand derived from vanillin and its transition metal complexes," *Journal of Pharmaceutical Sciences and Research,* vol. 9, no. 8, p. 1317, 2017.

[14] C. Lucarelli, A. Giugni, G. Moroso, and A. Vaccari, "FT-IR Investigation of Methoxy Substituted Benzenes Adsorbed on Solid Acid Catalysts," *The Journal of Physical Chemistry C,* vol. 116, no. 40, pp. 21308-21317, 2012.

[15] R. H. Georgieva, P. S. Vassileva, A. K. Detcheva, D. K. Voykova, T. I. Gerganova, and Y. Y. Ivanova, "Synthesis, characterization and adsorption properties of nanostructured hybrid materials modified by boron and zirconium," *Central European Journal of Chemistry,* vol. 10, pp. 1484-1494, 2012.

[16] K. Turhan, F. Sahbaz, and A. Güner, "A spectrophotometric study of hydrogen bonding in methylcellulose-based edible films plasticized by polyethylene glycol," *Journal of Food Science,* vol. 66, no. 1, pp. 59-62, 2001.

[17] H. H. Alkam, E. M. Atiyah, N. M. Majeed, and W. M. Alwan, "Cupper (ii) and mercury (ii) complexes with schiff base ligands from benzidine with isatin and benzoine: synthesis, spectral characterization, thermal studies and biological activities," *Systematic Reviews in Pharmacy,* vol. 12, no. 1, 2021.

[18] A. Isiyaku, I. T. Siraj, A. U. Maigari, and B. Magaji, "Synthesis, characterization and anti-bacterial activity of Schiff base and its mixed ligand complexes of Cr (II) and Co (II) containing vanillin and 2-aminophenol," ed: DUJOPAS, 2021.

[19] H. H. Mihsen, S. K. Abass, Z. M. Hassan, and A. K. Abass, "Synthesis, Characterization and Antimicrobial Activities of Mixed Ligand Complexes of Fe (II), Co (II), Ni (II) and Cu (II) Ions Derived from Imine of Benzidine and o-phenylenediammine," *Iraqi Journal of Science,* pp. 2762-2775, 2020.

[20] A. J. Abdul-Ghani and A. M. Khaleel, "Synthesis and characterization of new schiff bases derived from N (1)-substituted isatin with dithiooxamide and their co (II), Ni (II), Cu (II), Pd (II), and Pt (IV) complexes," *Bioinorganic Chemistry and Applications,* vol. 2009, 2009.

[21] H. A. G. Al-Halfi, W. A. Al-Masoudi, and A. A. Alrekabi, "Synthesis and physiological study of Schiff base derived from sulfanilamide and vaniline," *Basrah Journal of Veterinary Research,* vol. 19, no. 2, pp. 281-290, 2020.

[22] A. M. Al-Khazraji and R. A. Al Hassani, "Synthesis, characterization and spectroscopic study of new metal complexes form heterocyclic compounds for photostability study," *Sys Rev Pharm,* vol. 11, no. 5, pp. 535-555, 2020.

[23] M. Bogdan, C. G. Floare, and A. Pîrnau, "1H NMR investigation of self-association of vanillin in aqueous solution," in *Journal of Physics: Conference Series*, 2009, vol. 182, no. 1: IOP Publishing, p. 012002.

[24] A. Hassan, A. Osman Said, B. H. Heakal, A. Younis, M. Abdelmoaz, and M. Abdrabou, "Conventional and Microwave-Assisted Synthesis, Antimicrobial and Antitumor Studies of Tridentate Schiff Base Derived from O-vanillin and Phenyl Urea and its Complexes," *Advanced Journal of Chemistry-Section A,* vol. 3, no. 5, pp. 621-638, 2020.

[25] M. Al-Jeboori, H. Hasan, and L. A. Karim, "Synthesis and Spectroscopic Studies of Mixed Catechol-Salicylaldiminate Derivatives of Antimony (III) and Tin (IV)," *Ibn AL-Haitham Journal For Pure and Applied Science,* vol. 21, no. 4, pp. 80-90, 2017.

[26] A. E. Fadhil and A. K. Abbas, "Antioxidant, Antimicrobial and Spectroscopic Discussion of Guanine Azo Ligand with Cu (II) and Ag (I) Complexes," *Ibn AL-Haitham Journal For Pure and Applied Sciences,* vol. 36, no. 4, pp. 207-220, 2023.

[27] C. P. Manankandayalage, D. K. Unruh, and C. Krempner, "Boronic, diboronic and boric acid esters of 1, 8-naphthalenediol–synthesis, structure and formation of boronium salts," *Dalton Transactions,* vol. 49, no. 15, pp. 4834-4842, 2020.

[28] X. Li, X. Wang, S. Subramaniyan, Y. Liu, J. Rao, and B. Zhang, "Hyperbranched polyesters based on indole-and lignin-derived monomeric aromatic aldehydes as effective nonionic antimicrobial coatings with excellent biocompatibility," *Biomacromolecules,* vol. 23, no. 1, pp. 150-162, 2021.

[29] C. Martin, J. Ronda, and V. Cadiz, "Boron-containing novolac resins as flame retardant materials," *Polymer Degradation and Stability,* vol. 91, no. 4, pp. 747-754, 2006.

[30] S. Handayani, R. Arianingrum, and W. Haryadi, "Vanillin structure modification of isolated vanilla fruit (Vanilla planifolia Andrews) to form vanillinacetone," in *Proceedings of 14th Asian Chemical Congress*, 2011, pp. 252-257.

[31] A. Setyawati, T. D. Wahyuningsih, and B. Purwono, "Syntheses of novel pyrazolines as antibacterial agents from natural product vanillin," *Asian Journal of Chemistry,* vol. 29, no. 2, pp. 454-456, 2017.

[32] M. I. Afridi, M. Qasim, and A. Hussanan, "Second law analysis of dissipative flow over a riga plate with non-linear Rosseland thermal radiation and variable transport properties," *Entropy,* vol. 20, no. 8, p. 615, 2018.

[33] H. K. Naji, R. A. Al Hassani, and A. A. Balakit, "Synthesis, characterization, and biological screening of Co (II), Ni (II), Cu (II), Pd (II), and Pt (IV) complexes of a novel hydrazide–hydrazone ligand derived from gallic acid," *Journal of Pharmaceutical Negative Results,* vol. 13, no. 4, pp. 1152-1159, 2022.

[34] St Ed. McGraw-Hill Publ. Co. Ltd., New York, 1968.B.P. Lever, "Inorganic Electronic Spectroscopy" *Elsevier Publishing Co. Amsterdam-London, New York*" 1968.

[35] M. Medvidović-Kosanović, A. Stanković, M. Jozanović, M. Drulak, and M. Ilić, "Electrochemical and UV/VIS study of l-histidine and its complexes with cobalt and nickel," *Croatica Chemica Acta,* vol. 91, no. 4, pp. 421-426, 2018.

[36] A. Kumar, "Study on Magnetic Susceptibility of Co (ii) Complexes and Electronic Spectra of Co (ii) Complexes," *International Journal of Innovations in Engineering Research and Technology,* vol. 8, no. 12, pp. 88-92.

[37] W. A. Mahmoud, Z. M. Hassan, and R. W. Ali, "Synthesis and spectral analysis of some metal complexes with mixed Schiff base ligands 1-[2-(2-hydroxybenzylideneamino) ethyl] pyrrolidine-2, 5-dione (HL1) and (2-hydroxybenzalidine) glycine (HL2)," in *Journal of Physics: conference series*, 2020, vol. 1660, no. 1: IOP Publishing, p. 012027.

[38] R. Fouad, I. A. Shaaban, T. E. Ali, M. A. Assiri, and S. Shenouda, "Co (II), Ni (II), Cu (II) and Cd (II)-thiocarbonohydrazone complexes: spectroscopic, DFT, thermal, and electrical conductivity studies," *RSC advances,* vol. 11, no. 60, pp. 37726-37743, 2021.

[39] P. M. Reddy and C. Pasha, "Copper (II) Complexes of New Carboxyamide Ligands: Synthesis, Spectroscopic and Antibacterial Study."

[40] I. Ali, W. A. Wani, and K. Saleem, "Empirical formulae to molecular structures of metal complexes by molar conductance," *Synthesis and reactivity in inorganic, metal-organic, and nano-metal chemistry,* vol. 43, no. 9, pp. 1162-1170, 2013.